Pulse shaping in mode-locked fiber lasers by in-cavity spectral filter

Sonia Boscolo,[1,*] Christophe Finot,[2] Huseyin Karakuzu,[1] and Periklis Petropoulos[3]

[1]*Aston Institute of Photonic Technologies, School of Engineering and Applied Science, Aston University, Birmingham B4 7ET, UK*

[2]*Laboratoire Interdisciplinaire Carnot de Bourgogne, UMR 6303 CNRS-Université de Bourgogne, 9 avenue Alain Savary, BP 47870, 21078 Dijon Cedex, France*

[3]*Optoelectronics Research Centre, University of Southampton, Highfield, Southampton SO17 1BJ, UK*

**Corresponding author: s.a.boscolo@aston.ac.uk*

Received November 6, 2013; accepted November 28, 2013;
posted December 18, 2013 (Doc. ID 200845); published January 20, 2014

We numerically show the possibility of pulse shaping in a passively mode-locked fiber laser by inclusion of a spectral filter into the laser cavity. Depending on the amplitude transfer function of the filter, we are able to achieve various regimes of advanced temporal waveform generation, including ones featuring bright and dark parabolic-, flat-top-, triangular- and saw-tooth-profiled pulses. The results demonstrate the strong potential of an in-cavity spectral pulse shaper for controlling the dynamics of mode-locked fiber lasers. © 2014 Optical Society of America

OCIS codes: (140.4050) Mode-locked lasers; (320.5540) Pulse shaping; (070.2615) Frequency filtering.
http://dx.doi.org/10.1364/OL.39.000438

Passively mode-locked fiber lasers have generated major interest as an alternative to solid-state systems owing to improved simplicity, stability, and cost. In general, they rely on nonlinear processes to achieve mode-locking, and major steps forward in pulse energy and peak power performance have been made with the recent discovery of new nonlinear mechanisms of pulse generation [1], namely, dissipative solitons in all-normal-dispersion cavities and parabolic self-similar pulse (similariton) propagation [2–5]. These are qualitatively distinct from the well-known soliton and dispersion-managed soliton (stretched-pulse) regimes. Further, the possibility of triangular and parabolic pulse shaping in mode-locked fiber lasers using nonlinear dynamics was reported in [6]. In relation to the work presented here, a spectral filter was used in [3] to initiate the transition from similariton evolution in the gain fiber segment of the laser to soliton evolution in an anomalous-dispersion segment by undoing the spectral broadening of the amplifier similariton. A strong spectral filter that compensated for the broad pulse duration and bandwidth after the gain segment provided the main mechanism for seeding similariton evolution in the amplifier in the all-normal-dispersion cavity demonstrated in [4]. From a fundamental standpoint, fiber lasers provide convenient and reproducible experimental settings for the study of the dynamics of dissipative systems. Thus far, however, mode-locked fiber lasers have been relatively limited in terms of their reconfigurability, and achieving different output pulse characteristics generally involves significant changes to the physical layout of the cavity.

Spectral pulse shaping [7] is a technique that employs spectral manipulation of the intensity and phase components of a pulse in order to create the desired field distribution at the output of a mode-locked laser. It has been highly successful for applications in a number of fields [8,9]. However, since the pulse shaper is normally placed outside the laser cavity, it requires careful alignment between the wavelength of the shaping filter and the emission wavelength of the laser, and its control of the laser field is limited; the bandwidth of the filtered spectrum is determined by the bandwidth of the input spectrum, and manipulation of the in-cavity dynamics of the laser is not possible. In addition, the pulse shaper can only subtract power from the frequency components of the signal while manipulating its intensity, thereby potentially making the whole process extremely power inefficient. The inclusion of a pulse shaper into the cavity of a passively mode-locked fiber laser was recently demonstrated [10], allowing for tunability of the wavelength and operation at high repetition rates. In [11,12], the phase-filtering ability of an in-cavity pulse shaper was shown to enable precise control of the cavity dispersion of the laser as well as to change the output pulse train from bright to dark pulses. In this Letter, we take advantage of the amplitude- and phase-filtering ability of an in-cavity spectral pulse shaper to numerically show the possibility to achieve different pulse-shaping regimes in a mode-locked fiber laser. By changing the amplitude profile applied to the filter, we are able to create various output temporal waveforms of fundamental and practical interest, ranging from bright and dark parabolic profiles to a flat-top profile, and triangular and saw-tooth (asymmetric triangular) profiles [13].

The cavity configuration considered is a simple ring cavity as shown in Fig. 1. The gain is provided by a

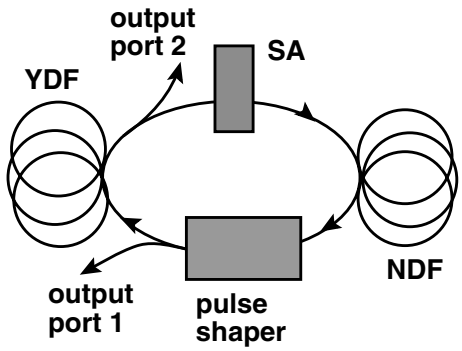

Fig. 1. Schematic of the laser. YDF, ytterbium-doped fiber; NDF, normally dispersive fiber; SA, saturable absorber.

1 m long segment of ytterbium-doped fiber (YDF) with normal group-velocity dispersion (GVD), while 6 m of single-mode fiber with normal GVD [normally dispersive fiber (NDF)] acts as the nonlinear element of the cavity. A saturable absorber (SA) element follows the gain fiber, and an amplitude and phase filter is placed between the passive fiber and the amplifier to realize the pulse shaping. Propagation within each section is modeled with a modified nonlinear Schrödinger equation for the slowly varying pulse envelope:

$$\psi_z = -\frac{i\beta_2}{2}\psi_{tt} + i\gamma|\psi|^2\psi + \frac{1}{2}g\left(\psi + \frac{1}{\Omega^2}\psi_{tt}\right), \quad (1)$$

where $\beta_2 = 25$ fs^2/mm is the GVD, and $\gamma = 0.005$ (Wm)$^{-1}$ is the coefficient of cubic nonlinearity for each fiber section [2]. The dissipative terms in Eq. (1) represent linear gain as well as a parabolic approximation to the gain profile with the bandwidth Ω corresponding to 40 nm full width at half-maximum (FWHM) bandwidth. The gain is saturated according to $g = g_0/(1 + W/W_0)$, where $g_0 = 35$ dB/m is the small-signal gain, which is nonzero only for the gain fiber, $W = \int dt|\psi|^2$ is the pulse energy, and $W_0 = 150$ pJ is the gain saturation energy determined by the pump power. The SA is given by a monotonically increasing transfer function $T = 1 - q_0/[1 + P(t)/P_0]$, where $q_0 = 0.9$ is the unsaturated loss, $P(t)$ is the instantaneous pulse power, and $P_0 = 150$ W is the saturation power. The filter is modeled by the spectral response $\hat{H}(\omega) = \hat{h}(\omega)\exp(i\beta_{2,\mathrm{acc}}\omega^2/2)$, where $\hat{h}(\omega)$ denotes the Fourier transform of a certain objective waveform function $h(t)$, and the spectral phase adds a specific amount of GVD to the cavity. By varying the curvature $\beta_{2,\mathrm{acc}}$ (in ps^2) of the parabolic phase function, we can control the net dispersion of the cavity. We consider the generation of five different amplitude functions in our study, which represent some examples of interesting optical waveforms. We use a bright parabolic pulse shaper with $h(t) = \sqrt{1 - (t/\tau)^2}\theta(\tau - |t|)$, $\tau = 1$ ps; a dark parabolic pulse shaper such that $h(t) = (1 - |t/\tau|)\theta(\tau - |t|)$ with $\tau = 1$ ps; a flat-top pulse shaper where $h(t) = \theta(\tau - |t|)$ with $\tau = 0.75$ ps; a triangular pulse shaper where $h(t) = \sqrt{1 - |t/\tau|}\theta(\tau - |t|)$ with $\tau = 1$ ps; and a saw-tooth pulse shaper where we define $h(t) = \sqrt{1 - t/\tau}$ in $t \in [0, \tau]$, $h(t) = 0$, otherwise, with $\tau = 2$ ps. Here $\theta(x)$ is the Heaviside function. Note that the spectral filter can be realized in a variety of ways, such as a fiber Bragg grating or even a programmable liquid crystal on silicon optical processor, which offers the additional advantage of being easily reconfigurable [14]; such devices are already commercially available. The output of the laser is monitored behind 70% and 10% couplers at the output of the pulse shaper and just after the gain segment, respectively. The numerical model is solved with a standard symmetric split-step propagation algorithm, and the initial field is a picosecond Gaussian temporal profile.

The solutions obtained for the different amplitude profiles applied to the filter and net GVD of 0.008 ps^2 are shown in Fig. 2. It is seen that the desired pulse shapes are obtained at the output of the filter. In the case of flat-top and saw-tooth waveform functions, because of the sharp edges of these pulse shapes, an additional Gaussian bandpass filter with a FWHM bandwidth of 2 THz is included in the pulse shaper to make the top of the resulting pulse ripple-free and to smooth the formed pulse shape, respectively. The generated parabolic and triangular pulses are nearly transform-limited, whereas the flat-top pulse features a small positive chirp.

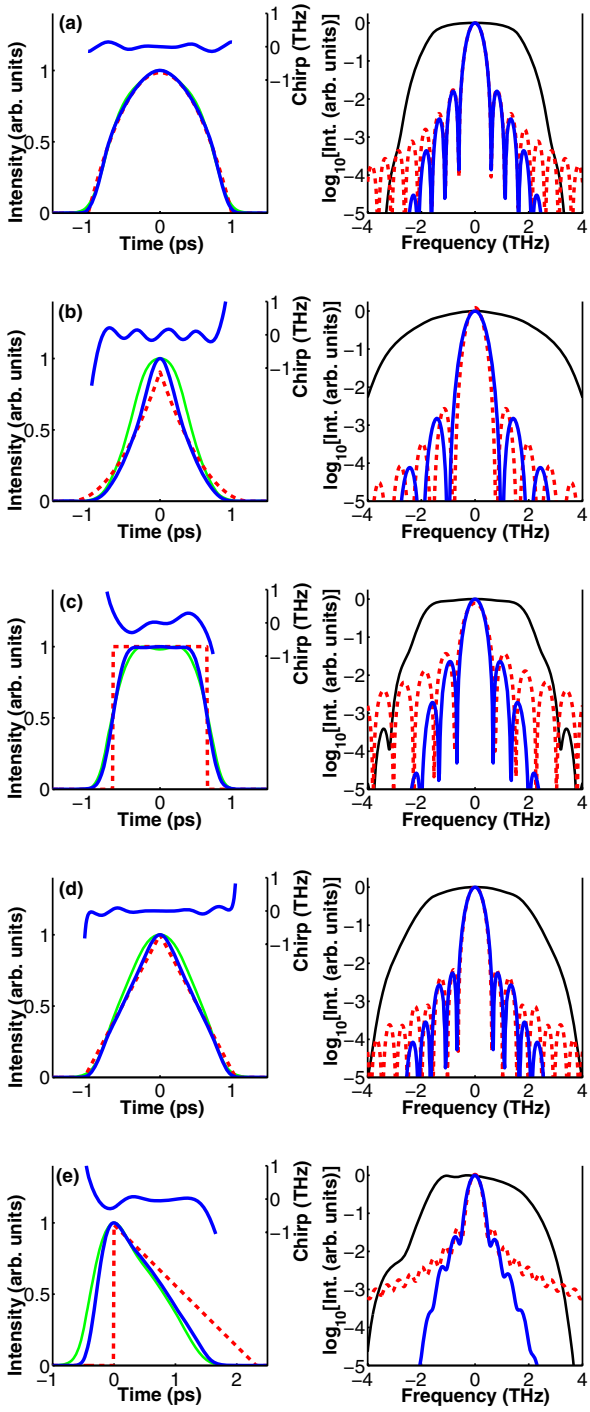

Fig. 2. Temporal intensity and chirp profiles (left) and spectral intensity profile (right) of the pulse after the pulse shaper (blue solid) for a (a) bright parabolic, (b) dark parabolic, (c) flat-top, (d) triangular, and (e) saw-tooth shaping function. Also shown are the target temporal and spectral profiles (dashed red), the temporal profiles at the exit of the gain fiber (green), and the spectral profiles before the pulse shaper (black).

We can also see from Fig. 2 that, as opposed to the chirp profile targeted by the filter, the chirp profile of the generated pulses may exhibit a small ripple. This indicates that generating pulses with a well-defined phase profile by use of the method proposed in this Letter is not as straightforward. Figure 2 also highlights that the temporal intensity profile imparted by the filter onto the pulse is reasonably well preserved after the amplification stage, where more energetic pulses can be extracted from the cavity.

The pulse evolution is illustrated by plots of the root-mean-square (rms) pulse duration and spectral bandwidth as functions of position in the cavity and quantified with the metric $M^2 = \int dt(|\psi|^2 - |\chi|^2)^2 / \int dt|\psi|^4$ (Fig. 3). Here ψ is the pulse being evaluated, and χ is a specific shape fit with the same energy and FWHM duration. The evolution shown for the triangular pulse-shaping regime is representative of those observed for the other shaping regimes too, in which the typical pulse parameters evolve in a closely similar fashion along the cavity, though small quantitative differences may exist. It is seen that during the short amplification stage there is no strong reshaping (which confirms the results in Fig. 2), and that most of the nonlinear dynamics occur in the long passive fiber. The peak nonlinear phase shift $\phi^{NL} = \int dz\gamma(z)P_0(z)$ (P_0 is the pulse peak power), which the pulse accumulates in one cycle around the cavity, is slightly greater than 9 rad, with ϕ^{NL} being slightly greater than 1 rad in the amplifier fiber and $\phi^{NL} \sim 8$ rad in the passive fiber. This indicates that the laser relies on rather strong nonlinearity combined with spectral filtering to stabilize the pulse in the cavity. The nonlinear evolution in the passive fiber is monotonic with the growth of temporal and spectral widths. The filter compensates for temporal and spectral broadening and cancels the large temporal phase accumulation in the fiber. The spectral breathing factor, defined as the ratio of the spectral FWHM at the input and the output of the filter, is approximately 6 in the example of Fig. 3. The principle of filtering a pulse in frequency and time due to the large chirp present has already been exploited to achieve new mode-locking regimes in fiber lasers [3,4]. In the present work, we extend this approach to more complex features. Because the nonlinearly broadened spectrum of the pulse at the output of the passive fiber is significantly wider than the filter's spectral response and fairly flat within the filter bandwidth (Fig. 2), it can be sliced without caring for the details of its structure. This is the enabling mechanism for the formation of pulses of any desired temporal shape at the output of the filter, determined by the filter's transfer function [15]. It is worth noting here that steady-state pulse shaping in an oscillator requires the generated pulse to fulfill the constraints imposed by the cavity, and formation of a self-consistent solution in the cavity is in general a nontrivial problem. Despite substantial research in this field, qualitatively new phenomena are still being discovered.

To gain a broader understanding of the laser dynamics, we investigated the effect of net dispersion on the laser response. Figure 4 shows results obtained for a triangular waveform function applied to the filter. It is seen that the best triangular pulses after spectral filtering are obtained for small values of normal net dispersion (~0.005 ps^2) and are close to transform-limited pulses. In the cases of bright parabolic and flat-top shaping functions (not shown in Fig. 4), we observed a shift of the dispersion range where the best parabolic and flat-top pulses can be generated toward small net anomalous values (~ – 0.01 ps^2) and slightly larger normal values (~0.02 ps^2), respectively. Note that the net dispersion is controlled by adjusting the transfer function of the pulse shaper; therefore, no physical change in the cavity is required in order to change the output from one pulse shape to another, provided that a programmable pulse shaper is used. The time-bandwidth product of the pulse remains close to the transform-limit for a triangular pulse (0.54) in the dispersion region being considered, which reveals that the potential of tuning the output pulse temporal duration through in-cavity linear chirping is minimal. This stems from the filtering process being

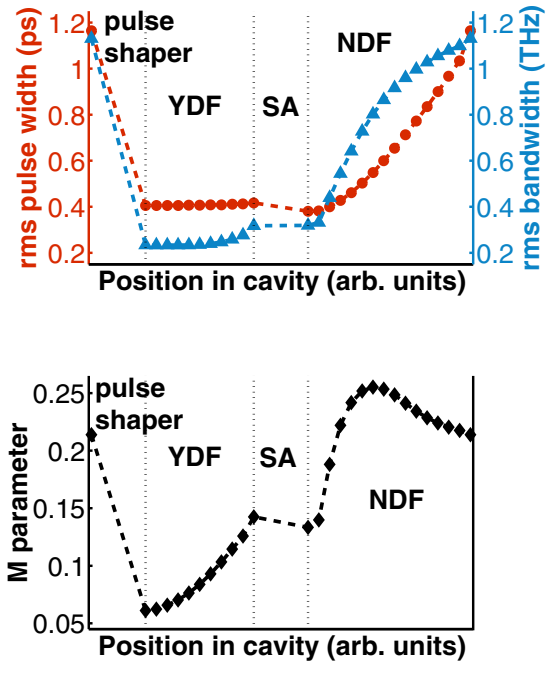

Fig. 3. Top: evolution of the rms temporal (red circles) and spectral (blue triangles) widths of the pulse along the cavity for the triangular pulse-shaping regime. Bottom: evolution of the misfit parameter to a triangular temporal shape (black rhombs).

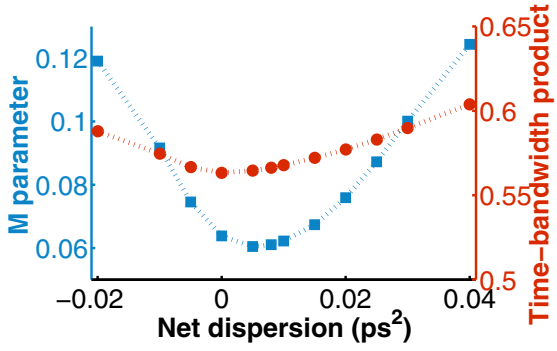

Fig. 4. Misfit parameter to a triangular temporal shape (blue squares) and time-bandwidth product (red circles) at the output of the pulse shaper versus net cavity dispersion.

used, i.e., slicing of a much broader spectrum, and indicates that one should act directly on the waveform function of the filter to control the output pulse width. This result is not surprising, in fact, as a triangular, parabolic, or flat-top temporal profile is rather sensitive to group delay.

In conclusion, we have numerically shown the operation of a passively mode-locked fiber laser in different pulse-shaping regimes, including bright and dark parabolic, flat-top, triangular, and saw-tooth waveform generations, depending on the amplitude profile of an in-cavity spectral filter. Using a spectral filter based on a programmable optical processor, one would be able to easily reconfigure the operation of the laser with a computer interface. From a practical viewpoint, the linear pulse-shaping approach used here is attractive because it provides a high degree of control over the output pulse shape of the laser to adjust its operation to different experimental requirements. Our work confirms the great potential of the concept of an in-cavity pulse shaper for controlling the dynamics and the output of mode-locked fiber lasers. Further, our results are of particular relevance with the high interest in the generation of specialized pulse waveforms for applications in optical signal processing and manipulation.

The authors would like to acknowledge support by the Leverhulme Trust (grant RPG-278). They also thank Dr. Miguel Preciado and Dr. Mykhaylo Dubov for useful discussions.

References

1. W. H. Renninger, A. Chong, and F. W. Wise, IEEE J. Sel. Top. Quantum Electron. **18**, 389 (2012).
2. F. Ö. Ilday, J. R. Buckley, W. G. Clark, and F. W. Wise, Phys. Rev. Lett. **92**, 213902 (2004).
3. B. Oktem, C. Ülgüdür, and F. Ö. Ilday, Nat. Photonics **4**, 307 (2010).
4. W. H. Renninger, A. Chong, and F. W. Wise, Phys. Rev. A **82**, 021805 (2010).
5. B. G. Bale and S. Wabnitz, Opt. Lett. **35**, 2466 (2010).
6. S. Boscolo and S. K. Turitsyn, Phys. Rev. A **85**, 043811 (2012).
7. A. M. Weiner, Rev. Sci. Instrum. **71**, 1929 (2000).
8. N. Dudovich, D. Oron, and Y. Silberberg, Nature **418**, 512 (2002).
9. T. Brixner, N. H. Damrauer, P. Niklaus, and G. Gerber, Nature **414**, 57 (2001).
10. J. Schröder, T. D. Vo, and B. J. Eggleton, Opt. Lett. **34**, 3902 (2009).
11. X. Yang, K. Hammani, D. J. Richardson, and P. Petropoulos, in *Conference on Lasers and Electro-Optics*, OSA Technical Digest (Optical Society of America, 2013), paper CM1I.1.
12. J. Schröder, S. Coen, T. Sylvestre, and B. J. Eggleton, Opt. Express **18**, 22715 (2010).
13. S. Boscolo and C. Finot, Int. J. Opt. **2012**, 159057 (2012).
14. M. Roelens, S. Frisken, J. Bolger, D. Abakoumov, G. Baxter, S. Poole, and B. Eggleton, J. Lightwave Technol. **26**, 73 (2008).
15. C. Finot and G. Millot, Opt. Express **12**, 5104 (2004).